IUST
Iran University of Science and Technology

Iranian Journal of Electrical and Electronic Engineering

Journal Homepage: ijeee.iust.ac.ir

Research Paper

Enhancement of Voltage/Frequency Stability in an Autonomous Micro Energy Grid with Penetration of Wind Energy Using a Parallel Fuzzy Mechanism

H. Shayeghi*(C.A.) and A. Younesi*

Abstract: The main objective of this paper is to model and optimize the parallel and relatively complex FuzzyP+FuzzyI+FuzzyD (FP+FI+FD) controller for simultaneous control of the voltage and frequency of a micro-grid in the islanded mode. The FP+FI+FD controller has three parallel branches, each of which has a specific task. Finally, as its name suggests, the final output of the controller is derived from the algebraic summation of the outputs of these three branches. Combining the basic features of a simple PID controller with fuzzy logic that leads to an adaptive control mechanism, is an inherent characteristic of the FP+FI+FD controller. This paper attempts to determine the optimal control gains and Fuzzy membership functions of the FP+FI+FD controller using an improved Salp swarm algorithm (ISSA) to achieve its optimal dynamic response. The time-domain simulations are carried out in order to prove the superb dynamic response of the proposed FP+FI+FD controller compared to the PID control methods. In addition, a multi-input-multi-output (MIMO) stability analysis is performed to ensure the robust control characteristic of the proposed parallel fuzzy controller.

Keywords: Fuzzy Logic, Micro Energy Grid, Voltage Control, Frequency Control, MIMO Stability.

1 Introduction

1.1 Motivation

ENERGY production is one of the main causes of environmental problems, including air pollution and global warming. Meanwhile, a significant share of this pollution is related to the production of electrical energy. Because in various aspects of human life it has a wide range of uses. For this reason, green electricity production has been considered as a way to mitigate the effects of burning fossil fuels for power generation [1]. The development of renewable energies (REs) such as wind and photovoltaic and the other sources raised the concept of micro energy grids (MEG) that were created to integrate these resources together and with the main network [2]. As a base definition, the MEG is a small scale electrical network with a specific electrical boundary, which is able to supply its loads when it is disconnected from the main network [3]. However, renewable energy sources along with environmental benefits impose many technical limitations on the MEG.

Voltage and frequency stability, reliability in supplying loads and power quality are serious challenges that are caused due to renewable energy sources' uncertain output [4]. Given these issues, the need for a targeted, adaptive and, of course stable, control system to address these challenges has always been a concern for researchers. For this reason, this paper tries to design this control system to enhance the stability of the voltage and frequency of an autonomous MEG using an improved Salp swarm algorithm and the fuzzy logic mechanism.

1.2 Literature Review

Since with the increasing attendance of distributed generations (DGs) in power systems, the total inertia of

Iranian Journal of Electrical and Electronic Engineering, 2020.
Paper first received 25 May 2019, revised 13 November 2019, and accepted 29 November 2019.
* The authors are with the Electrical Engineering Department, Faculty of Engineering, University of Mohaghegh Ardabili, Ardabil, Iran.
E-mails: hshayeghi@gmail.com and younesi.abdollah@gmail.com.
Corresponding Author: H. Shayeghi.

the whole power system is reduced, and therefore, the voltage and frequency of the system are more likely to fluctuate [5]. Thus, in recent years, the control of frequency and voltage stability of MEGs has attracted more attention from researchers due to the increasing development of renewable energy sources with variable and randomized outputs [6, 7]. Zhao *et al*. [8], based on the output regulation theory, and battery storage with fast response, have designed a controller to improve the frequency fluctuations and the voltage stability of the MEG. They have been trying to improve some weaknesses of droop-based controllers, including settling time and poor transient performance. A control scheme based on the method of voltage-current and voltage-voltage drop component for the controlling of the voltage and current of the MEG is presented in [9]. The proposed method calculates the output impedance of the source subsystem along with the converter's dynamics and analyzes the stability of the MEG when supplying constant loads. First, the paper examines the stability effects of the key parameters such as loss coefficients, local loop dynamics and the number of sources, and then compares the current and voltage states from a stability perspective. Power control in a grid-connected PV/Fuel Cell/Battery hybrid power generation system in a microgrid is considered in [10]. Reference [10] has used SIMULINK/SIMPOWER to model the system and simulate the power flow control strategy. PV, fuel cell and battery subsystems with power electronic converters are accurately modeled. Then control strategies are designed for power electronic converters based on the classic and sliding mode control. Authors in [11] have presented a robust design of an adaptive fuzzy P-PID controller for a microgrid with different types of uncertainties and power units to enhance the frequency deviation damping caused by microgrid performance under unexpected conditions. A multi-objective Chaotic Gravitational Search Algorithm algorithm has been used to optimally tune the fuzzy set variables in the suggested fuzzy controller. Based on two conflicting objective functions in time and frequency domains, the proposed design problem is converted to a multi-objective optimization problem over a wide range of loading conditions. A detailed model of the flywheel energy storage system (FESS) has been presented in [12] and several control strategies such as PQ control, V/f control and two complementary controllers have been introduced and applied to the FESS. The complementary controllers include a PI controller and fuzzy controller respectively that change the no-load frequency of the FESS in V/f control mode. Authors in [13], have suggested a low voltage feedback controller, which is second-order at the local level voltages. With the help of this method, it is possible to use circuit theory analysis techniques in a closed-loop system. In [14], a new fuzzy logic control method, along with energy storage, is used to control the frequency and voltage of a MEG in the island mode. In this paper, battery storage is used to improve the frequency fluctuations and the ultra-capacitor for the voltage stability of the MEG. A distributed secondary control structure for power electronic-based AC MEG has been proposed in [4]. In the suggested method in [4], a model predictive control strategy is applied in the inner primary control level in order to regulate the voltage of power converters. The result is that by using the proposed method for paralleled voltage source converters the voltage regulation of converters is enhanced with a quick transient response. In [15], a traditional PID controller is designed to control the voltage and frequency of the MEG, using the GA toolbox of MATLAB. In addition, a superconductor magnetic energy system is placed to improve the dynamic performance of the system.

1.3 Contribution

Fuzzy logic-based controllers are undoubtedly the most successful applications of fuzzy systems. The ever-increasing use of the fuzzy logic (FL) based methods to enhance the efficiency of industrial processes is undeniable. In this condition, it is necessary to analyze this kind of controllers more mathematically in the simulation environment in order to achieve their best dynamic response. Controlling strategies that are successfully developed in most industrial applications, with the inherent vital features such as adaptability and robust against system changes and parameter uncertainties [16-21]. Therefore, in this paper, a parallel fuzzy logic-based control strategy called FP+FI+FD controller [22] is designed for simultaneous voltage and frequency control of an autonomous MEG. As its name indicates, the FP+FI+FD controller is consists of three parallel branches i.e. fuzzy P, fuzzy I, and fuzzy D. Each of these wings performs a specific duty independent of the other parts. Increasing the speed of the system, transient stability, and removing the steady-state error are the main tasks of FP, FI, and FD controllers, respectively. Finally, the control output of FP+FI+FD controller is obtained from the algebraic summation of FP, FI, and FD parts [22]. The proposed FP+FI+FD controller has a robust, adaptive, and very quick behavior thanks to its flexible structure that combines the advantages of the traditional PID controller along with fuzzy logic characteristics. Although the FP+FI+FD controller has a high degree of freedom due to its large number of control parameters (9 control parameters), on the other hand, it is difficult to determine the optimal values of these parameters. Therefore, the use of heuristic optimization algorithms that have a high speed and precision in finding the optimal solution for optimization problems is recommended to determine the optimal parameters of FP+FI+FD [21, 23]. The Salp swarm algorithm (SSA) is a bio-inspired optimization algorithm that

mathematically models the movement of Salp individuals toward the food location (the optimal solution) [24]. In this paper, an improved version of SSA called ISSA is considered for determining the optimal values of the control parameters of the proposed FP+FI+FD controller. The improvements have been made in changing the method for switching between the exploration and exploitation phases of the SSA algorithm. In order to gain the best dynamic performance of the FP+FI+FD in this paper, in addition to the nine control parameters, the span of the fuzzy membership functions is also optimized using the suggested ISSA algorithm. Finally, in order to evaluate the dynamic response of the proposed FP+FI+FD controller, a test MEG is considered and simulated mathematically using MATLAB/SIMULINK software. Then, by challenging the system status by the scenario of a three-phase fault, the performance of the proposed FP+FI+FD controller compared with the traditional PID controller (both are optimized by ISSA) is examined. The simulation results reveal that the proposed control strategy is robust and can cope with the system nonlinearities more efficient compared to the PID controller. Further, according to the results provided in [25], the multi-input-multi-output stability analysis is performed for the proposed test MEG equipped with FP+FI+FD voltage and frequency controllers. As the results show, the FP+FI+FD voltage and frequency controllers that are placed in the MEG ensure the voltage and frequency stability of the whole system.

The main novel investigations of the paper are:

1) To design an optimal parallel FP+FI+FD controller for voltage and frequency stability of a micro energy grid.
2) To utilize an improved version of the Salp swarm algorithm for finding the best values of the controller parameter and fuzzy membership function intervals.
3) To perform a MIMO stability analysis in the proposed micro energy grid equipped with a fuzzy logic-based FP+FI+FD controller.

2 Modeling Methodologies

A micro energy grid (MEG) is a relatively small power grid, comprising energy resources and consumers with a distinct electric boundary, which is able to supply it's loads when it is connected and separated from the main grid [26]. Generally, a MEG has different energy resources, including diesel engine generators (DEG), combined heat and power (CHP) units, and renewable energy resources(RER) such as wind turbine generator (WTG) and photovoltaic (PV) [27]. The MEG that is considered in this paper consists of three fixed-speed stall-regulated WTGs, a CHP with three gas turbine generators (GTG), and 10 loads [28]. In the following, the mathematical model of each element in the considered MEG is provided in detail.

2.1 WTG Model

The output power of WTG in a discrete-time environment with the sampling time of T seconds in instance n can be obtained using (1) as follows [29]:

$$P_{WTG}(nT) = \frac{1}{2}\rho\pi R^2 C_P(\lambda(nT),\beta(nT))V(nT)^3 \quad (1)$$

where R indicates the rotational radius, ρ is the air density, $C_P(\lambda, \beta)$ refers to the WTG power coefficient, λ is the tip speed ratio that is a function of the turbine rotational speed, β is the pitch angle of the turbine blades and V denotes the wind speed. The output torque of WTG is calculated by (2).

$$T_{WTG}(nT) = \frac{P_{WTG}(nT)}{\omega_r} = \frac{1}{2\lambda}\rho\pi R^3 C_P(\lambda(nT),\beta(nT))V(nT)^2 \quad (2)$$

When a torque of T_{WTG} received by turbine blades, it will be rotating with the speed of ω_r. By using forward difference method with the non-zero spacing value of h, Eqs. (3)–(5) can express the wind turbine and generator dynamics properly [29].

$$T_{WTG}(nT) - T_m(nT) = J_r\frac{\Delta_h^2[\theta_r](n)}{h^2} + C_r\frac{\Delta_h[\theta_r](n)}{h} + K_r\theta_r \quad (3)$$

$$T_p(nT) - T_e(nT) = J_g\frac{\Delta_h^2[\theta_g](n)}{h^2} + C_g\frac{\Delta_h[\theta_g](n)}{h} + K_g\theta_g \quad (4)$$

$$T_p\frac{\Delta[\theta_g](n)}{h} = T_m\frac{\Delta[\theta_r](n)}{h} \quad (5)$$

where T_m, T_p, T_e refer to the mechanical, generator, and electrical load torques, respectively. In addition, J, C, and K are inertia moment, damping factor and torsion stiffness factor of the shaft, respectively. Fig. 1 shows the general energy conversion process in WTG unit.

2.2 CHP Units Model

Regarding this fact that the synchronous generator performs power generation in the CHP unit, thus, for the modeling of the CHP units, the dynamical model of synchronous generator equipped with the excitation system is used. Equations (6)–(10) describes the synchronous generator dynamics [30]. Figure 2 shows the general schematic of the CHP.

$$\frac{\Delta[\delta](n)}{h} = \omega_B(S_m - S_{mo}) \quad (6)$$

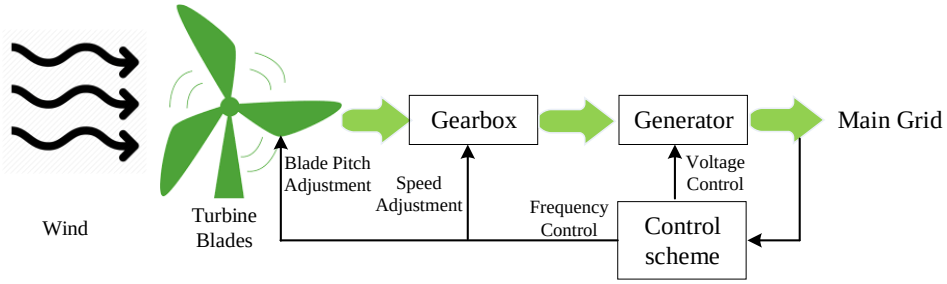

Fig. 1 General energy conversion process in WTG.

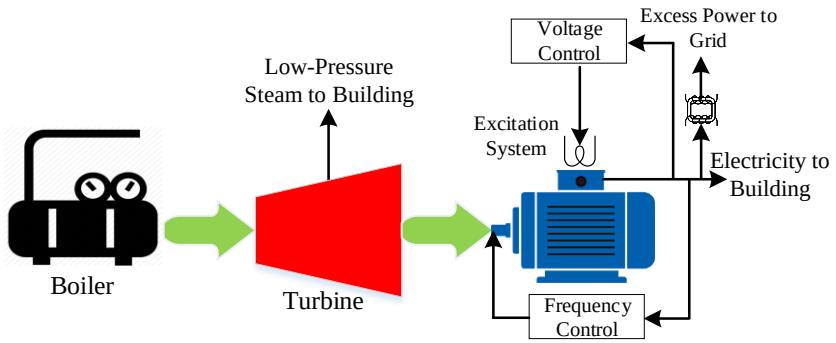

Fig. 2 General energy conversion process in CHP.

$$\frac{\Delta[S_m](n)}{h}=\frac{1}{2H}[-D(S_m-S_{mo})+T_m-T_e] \quad (7)$$

$$\frac{\Delta[E'_q](n)}{h}=\frac{1}{T'_{do}}[-E'_q+(x_d-x'_d)i_d+E_{fd}] \quad (8)$$

$$\frac{\Delta[E'_d](n)}{h}=\frac{1}{T'_{do}}[-E'_d-(x_q-x'_q)i_q] \quad (9)$$

$$T_e=E'_d i_d+E'_q i_q+(x'_d-x'_q)i_d i_q \quad (10)$$

2.3 Reduced Y_{bus} Modelling

It is important to realize that in dynamic analysis, the impact of loads, capacitor and reactor compensators entered in the modeling as a constant admittance, which can be calculated using (11) [30].

$$y_i=\frac{P_i-jQ_i}{V_{base}} \quad (11)$$

where P_i, Q_i, and V_{base} are the active power, reactive power at bus i, and the base voltage, respectively. The parameter y_i is used as a shunt admittance in the corresponding bus and is entered into transmission admittance matrix Y_{bus}. The size of Y_{bus} can be reduced by removing load buses from the original Y_{bus}. In this method, the impact of non-generator buses is transferred into generator buses using (12) [31].

$$Y_{bus}=\begin{bmatrix}Y_{GG} & Y_{GN}\\ Y_{NG} & Y_{NN}\end{bmatrix}\rightarrow Y_{bus}^{red}=Y_{GG}-Y_{GN}\times Y_{NN}^{-1}\times Y_{NG} \quad (12)$$

As an illustration, Fig. 3 shows the final modeling stage, in which the dynamics of the micro energy grid can be evaluated.

3 Parallel Fuzzy Logic Mechanism

The fundamental structure of a fuzzy logic controller (FLC) consists of three parts. The structure that is shown in Fig. 4 includes fuzzification, rule-based interface, and defuzzification. Each of these cascade sections has its own functionality. The function of fuzzification is to create linguistic data based on the numerical inputs that are suited to decision-making based on the rules. In the next stage, the fuzzy sets created in the previous section are used to create fuzzy outputs according to the fuzzy rule table. Finally, defuzzification is used to obtain the final numerical outputs [16]. Generally, the input and output signals of FLC must be modulated using proper gains [21].

The proposed FLC in this paper is called FP+FI+FD and consists of three parallel branches. Each branch has its own duty that is not in contradiction with the other parts and the overall objective of the controller. Figure 5 shows the block diagram of the FP+FI+FD controller. Where $T>0$ is the sampling time, $y_{SP}(nT)$ is the reference set-point, $y(nT)$ is the process variable, $e(nT)=y_{SP}(nT)-y(nT)$ is the error signal, and $u_{P+I+D}(nT)$ is the output of the parallel FP+FI+FD controller [21]. As the name indicates, this control strategy consists of fuzzy proportional (FP), fuzzy derivative (FD) and fuzzy integral (FI) controllers. The functionality of the FP part is to make the system faster. Also, in order to eliminate the fast change and large overshoots in control inputs, and steady-state error, FD and FI sections are suggested, respectively. The parallel FP+FI+FD control action can be obtained by the algebraical sum of fuzzy P control,

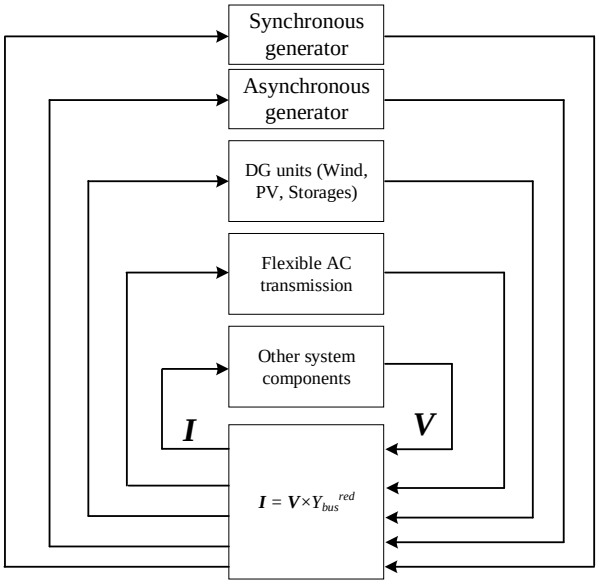

Fig. 3 Y_{bas}^{red} based modeling of MEG.

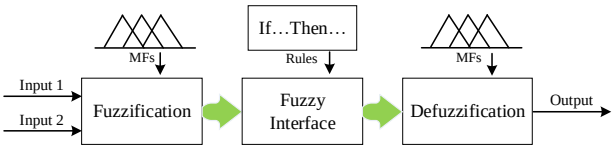

Fig. 4 Fuzzy logic based controller.

fuzzy I control and fuzzy D control actions, simultaneously [32]. The resultant control action is as follows [23]:

$$u_{P+I+D}(nT) = K_p u_P(nT) + u_I(nT - T) + K_I \Delta u_I(nT) - u_D(nT - T) + K_D \Delta u_D(nT) \quad (13)$$

where $u_P(nT)$ and K_p are the FP controller action and gain, $\Delta u_I(nT)$ and K_I are the incremental control action and gain of FI controller, $\Delta u_D(nT)$ and K_D are the incremental control action and gain of FD controller. Due to increasing the parameter in the FP+FI+FD controller, the degree of freedom is increased than the conventional PID controller and then the user has more flexibility to achieve the desired level of system response [21].

It can be seen from Fig. 3, the FP+FI+FD controller has three independent fuzzy structures. Each of these fuzzy structures has two inputs and one output. The membership function of the inputs and output of these fuzzy systems are similar and shown in Fig. 6 [32].

The optimal regulation of fuzzy rules is a challenge that researchers believe that engineering knowledge and understanding the dynamics of the studied system are the most important factors in achieving optimal fuzzy rules [32]. Since the proposed FP+FI+FD controller has three distinct fuzzy structures, the set of fuzzy rules for each of them are tabulated in Table 1 and illustrated in Fig. 7. The rules are defined based on the engineering knowledge and the specific tasks of each fuzzy structures [32].

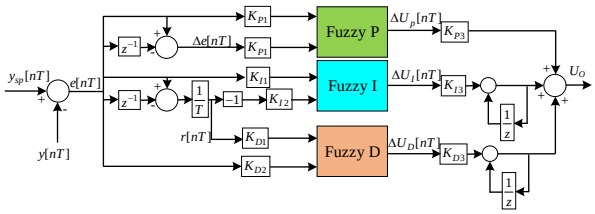

Fig. 5 The FP+FI+FD structure.

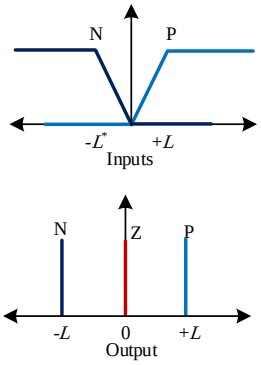

* L is an adjustable parameter that can be optimally determined for each specific control process.

Fig. 6 The FP+FI+FD controller's input/output MFs.

Table 1 Fuzzy rules of the FP+FI+FD controller.

		Input#2					
		Fuzzy P		Fuzzy I		Fuzzy D	
		N	P	N	P	N	P
Input #1	N	Z	P	N	Z	Z	P
	P	N	Z	Z	P	N	Z

4 Optimization

As shown in Figs. 3 and 4, the FP+FI+FD controller has ten adjustment parameters, namely K_{P1}, K_{P2}, K_{P3}, K_{I1}, K_{I2}, K_{I3}, K_{D1}, K_{D2}, K_{D3}, and L. Dynamic performance of the controller is largely influenced by the optimal setting of these parameters [23]. It should be noted that the increase in the number of adjustment parameters, although increases the degree of freedom of the controller, also makes it almost impossible to adjust them optimally using manual and mathematical-based methods [21]. Therefore, researchers have resorted to meta-heuristic optimization algorithms such as particle swarm [33], Genetic [34], and other similar methods in order to optimally tune such a kind of complex controllers. For this reason, in this paper, the Improved Salp swarm algorithm (ISSA) [24] is used to optimally adjust the control parameters of the FP+FI+FD to achieve the best dynamic response.

4.1 Improved Salp Swarm Algorithm

Salp swarm algorithm is a particle-based optimization

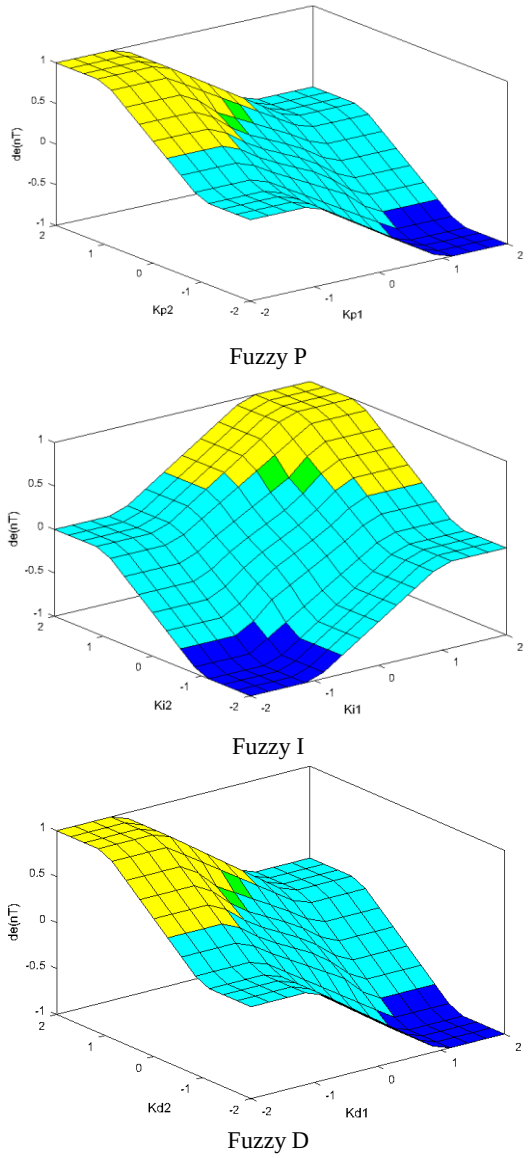

Fig. 7 The surface view of the fuzzy rules of FP+FI+FD controller.

method, which mathematically models the movement of Salp particles toward the food location that is considered as the best solution. In order to cope with multi-parameter optimization problems an *n*-dimensional space is suggested, where *n* is the number of variables to be optimized [24]. In each iteration, the particle with the best position (nearest to the food location) is selected as the leader of the other particles and Eq. (14) update its position.

$$X_j^1 = \begin{cases} F_j + c_1((ub_j - lb_j)c_2 + lb_j) & c_3 \geq 0 \\ F_j - c_1((ub_j - lb_j)c_2 + lb_j) & c_3 < 0 \end{cases} \quad (14)$$

where X_j^1 is the first leader, F_j is food location, ub_j and lb_j are the upper and lower bounds of the parameters all in *j*-th dimension. c_1, c_2, and c_3 are random numbers. Equation (15) calculates the parameter c_1, which is the most important parameter of SSA because it balances the exploration and exploitation phases. Since the number of adjustment parameters is high in this paper, a trigonometric equation that is given by (16) is suggested for calculating c_1.

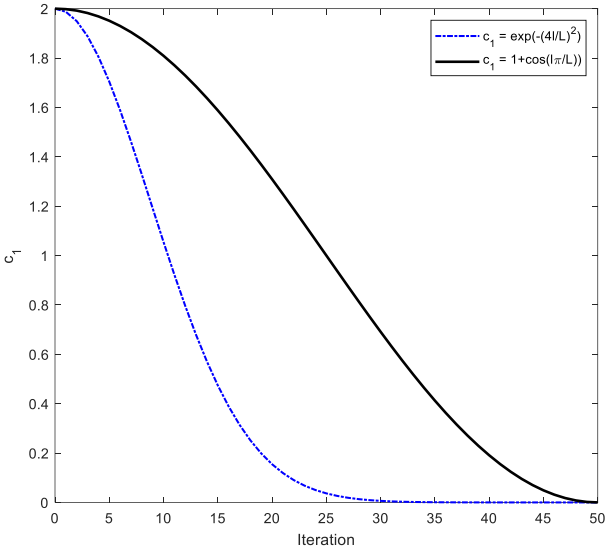

Fig. 8 The difference between the values of parameter c_1 in [24] (dash-dotted) and this paper (solid).

$$c_1^{old} = 2e^{-(\frac{4l}{L})^2} \quad (15)$$

$$c_i^{new} = 1 + \cos(\frac{l\pi}{L}) \quad (16)$$

where l is the current iteration and L is the maximum number of iterations. Parameters c_2 and c_3 are determined using normal distribution in the range [0 1]. As shown in Fig. 8, by replacing (15) with (16), the algorithm has more opportunity to search the space in order to find the optimal solutions. The improved Salp swarm algorithm explores the search environment more accurately, therefore, due to a large number of control parameters in the proposed control strategy, it can find more accurate optimal solutions.

According to Newton's displacement law, the position of the imitative Salp individuals is derived by (17).

$$X_j^i = \frac{1}{2}at^2 + v_0 t \quad (17)$$

where i>2, X^i_j is the position of *i*-th Salp particle in *j*-th dimension, t refers to time, v_0 is the initial speed, a=v_{final}/v_0 which $v = (x - x_0) \times t^{-1}$. In the concept of optimization, time is equivalent to iteration and the space between the iterations is 1. With this in mind and proposing 0 for the initial speed of all individuals, Eq. (17) can be rewritten as (18). More detail about the ISSA can be found in [24]. Fig. 9 shows the flowchart of the ISSA.

$$X_j^i = \frac{1}{2}(X_j^i + X_j^{i-1}) \quad (18)$$

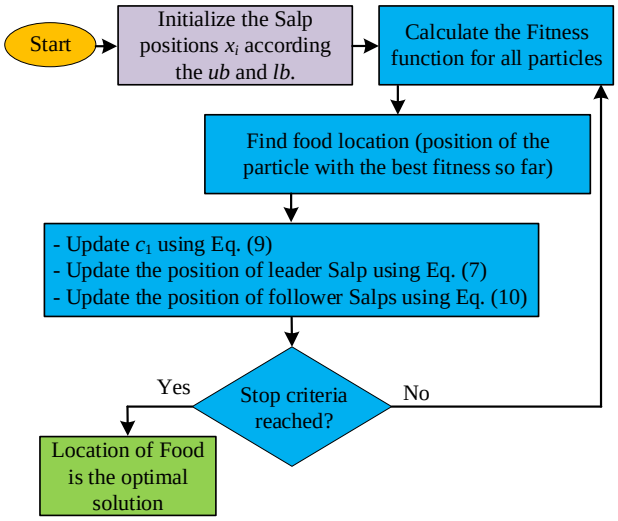

Fig. 9 The simplified flowchart of ISSA.

4.2 Problem Formulation

It is clear that simultaneously design of the controller for all the power sources in a micro energy grid is complex and non-economic. Especially when the production capacity of some resources is much less than the other ones. In this situation, the design of the controller for resources with higher production capacity can be both technically and economically desirable. Therefore, with this in mind, the controller design for wind generators is neglected in this paper, and in contrast, two controllers for CHP generation units are simultaneously designed for voltages and frequency. Since it is assumed that all the CHP units are identical, voltage and frequency controllers of all units are considered equal. Given these simplistic assumptions, two controllers must be designed to regulate the voltage and frequency of the micro energy grid simultaneously. For this purpose, the discrete-time objective function of (19) is suggested, which simultaneously evaluates the quality of the voltage and frequency of the micro energy grid.

$$J=\sum_{n=0}^{\frac{40}{T}} nT\left[\left(\Delta f_{CHP1}(nT)+\Delta f_{CHP2}(nT)+\Delta f_{CHP3}(nT)\right)\right.$$
$$\left.+\Upsilon\times\left(\Delta V_{CHP1}(nT)+\Delta V_{CHP2}(nT)+\Delta V_{CHP3}(nT)\right)\right] \quad (19)$$

where n is an integer, T is sampling time, and Υ is a weight constant. Consequently, the final optimization problem that includes the objective function and parameter constraints is given by (20).

minimize J

subject to:

$$K_{P1,f}^{\min} < K_{P1}^{f} < K_{P1,f}^{\max}$$
$$K_{I1,f}^{\min} < K_{I1}^{f} < K_{I1,f}^{\max}$$
$$K_{D1,f}^{\min} < K_{D1}^{f} < K_{D1,f}^{\max}$$
$$K_{P2,f}^{\min} < K_{P2}^{f} < K_{P2,f}^{\max}$$
$$K_{I2,f}^{\min} < K_{I2}^{f} < K_{I2,f}^{\max}$$
$$K_{D2,f}^{\min} < K_{D2}^{f} < K_{D2,f}^{\max}$$
$$K_{P3,f}^{\min} < K_{P3}^{f} < K_{P3,f}^{\max}$$
$$K_{I3f}^{\min} < K_{I3}^{f} < K_{I3,f}^{\max}$$
$$K_{D3,f}^{\min} < K_{D3}^{f} < K_{D3,f}^{\max}$$
$$K_{P1,v}^{\min} < K_{P1}^{v} < K_{P1,v}^{\max}$$
$$K_{I1,v}^{\min} < K_{I1}^{v} < K_{I1,v}^{\max}$$
$$K_{D1,v}^{\min} < K_{D1}^{v} < K_{D1,v}^{\max}$$
$$K_{P2,v}^{\min} < K_{P2}^{v} < K_{P2,v}^{\max}$$
$$K_{I2,v}^{\min} < K_{I2}^{v} < K_{I2,v}^{\max}$$
$$K_{D2,v}^{\min} < K_{D2}^{v} < K_{D2,v}^{\max}$$
$$K_{P3,v}^{\min} < K_{P3}^{v} < K_{P3,v}^{\max}$$
$$K_{I3v}^{\min} < K_{I3}^{v} < K_{I3,v}^{\max}$$
$$K_{D3,v}^{\min} < K_{D3}^{v} < K_{D3,v}^{\max}$$
$$L_{\min}^{f} < L^{f} < L_{\max}^{f}$$
$$L_{\min}^{v} < L^{v} < L_{\max}^{v} \quad (20)$$

In this paper, the range of the control parameters and adjustable parameter L is considered in the range of [-1 1] and [0.1 1000], respectively.

4.3 Micro Energy Grid Under Study

A typical European distribution power system owned by Himmerlands Elforsyning located in Aalborg, Denmark with high penetration of DG units is considered in this paper [28]. It consists of three fixed-speed stall-regulated wind turbine generators, a combined heat and power plant (CHP) with three gas turbine generators (GTG) namely CHP1, CHP2, and CHP3, and 10 loads. It is assumed the WTG units have the capacitor banks for necessary compensation and they operate close to the unity power factor. In the considered operating point, the production of 2.5MW, 2.8MW, and 2.8MW are assumed for CHP1, CH2, and CHP3, respectively and 0.08MW for each WTG. Fig. 10 shows the single line diagram of the proposed MEG and locations of load and power plants [28]. The Information that is used to model the test system has been taken from [28].

4.4 Optimization Results

Eventually, the constraint optimization problem (20) is solved using the improved Salp swarm algorithm (ISSA) and results are tabulated in Table 2. It should be noted that one of the main features of the SSA (and thus ISSA) algorithm is that it has no specific initial parameter to adjust. Therefore, here, the number of

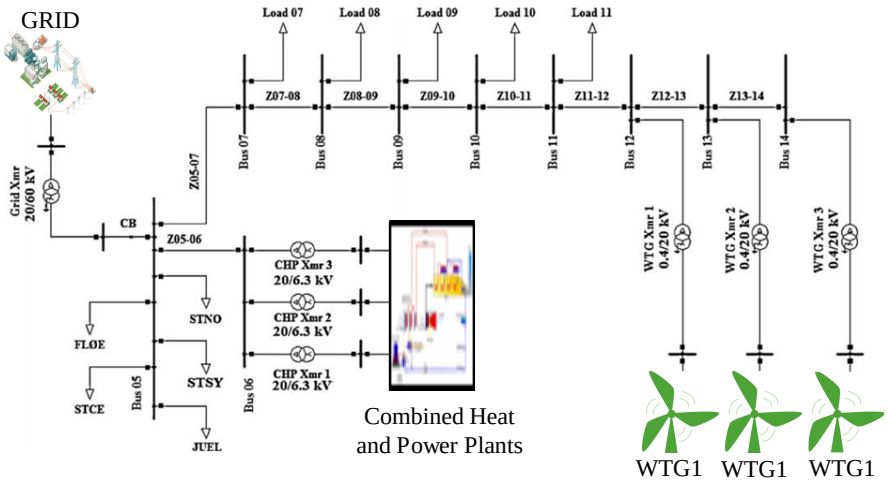

Fig. 10 Single-line diagram of the proposed micro energy grid [28].

Table 2 Optimal parameter of different control mechanisms obtained by ISSA.

FP+FI+FD										
Controller Type	K_p	K_{p1}	K_{p2}	K_i	K_{i1}	K_{i2}	K_d	K_{d1}	K_{d2}	L
Frequency	0.93229	0.54834	0.640727	0.154274	0.250193	0.293543	0.089966	0.125711	0.094457	683.85272
Voltage	0.245244	0.476872	0.349897	0.100977	0.116915	0.077633	0.012365	0.010279	0.016528	725.9996
PID										
Controller Type	K_p			K_i			K_d			
Frequency	0.48452			0.15012			0.002358			
Voltage	0.08529			0.02945			0.00112			

initial Salp particles and the maximum number of iterations are considered equal to 30 and 50, respectively, to solve the proposed 20-dimensional optimization problem. It should be noted that in order to prove the superiority of the proposed controller compared to classical methods, a traditional PID controller is used. The dynamic behavior of the PID controller is expressed using (21).

$$U_{PID} = K_p \Delta e(nT) + K_I \sum \Delta e(nT) + K_D \frac{\Delta_h}{h} [\Delta e(nT)] \quad (21)$$

5 Results and Discussion

As can be seen in Fig. 11, it is clear that the performance of the improved version of the SSA optimization algorithm is superior to that of its typical version for optimizing the parameters of the FP+FI+FI controller in the test MEG. For this reason, in this paper, ISSA has been used to determine the optimal fuzzy logic control parameters. In order to illustrate the dynamic response of the FP+FI+FD controller compared to the customary PID control method, the proposed MEG is mathematically modeled using the MATLAB/Simulink 2018 environment. Then, the scenario of the occurrence of a three-phase fault at bus 7 is defined to challenge the performance of the control methods in maintaining the voltage and frequency stability of the MEG.

5.1 Results

In order to simulate the MEG, reduced Y_{bus} matrix must first be calculated. Then, at the given operating points for the generation units and loads, the load flow analysis is done and the initial conditions are calculated [35]. The reduced Y_{bus}, the results of Newton-Raphson load flow and initial condition calculations are provided in the Appendix. The frequency oscillations of CHP and WTG units are plotted in Figs. 12 and 13, respectively.

According to Figs. 12 and 13, both control strategies have the ability to eliminate the oscillations of frequency deviations of the generation units. However, it's clear that the FP+FI+FD controller has a tremendous dynamic efficiency compared to a classical PID controller. FP+FI+FD controller has an excellent dynamic performance thanks to its flexible structure, which integrates the fuzzy logic adaptive property with the speed and precision of the PID controller. In order to more highlight the capabilities of the FL-based FP+FI+FD controller, the voltage deviation of the generation buses are shown in Figs. 14 and 15. Under the conditions of the same fault, the amplitude of the voltage fluctuations is much smaller than the frequency fluctuations. In these circumstances, the superiority of

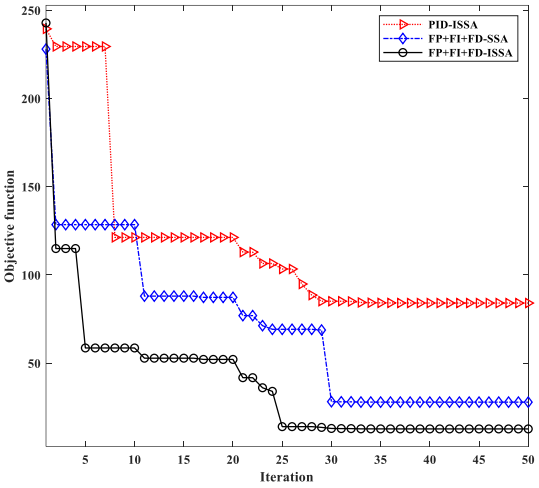

Fig. 11 Convergence of the objective function for different control mechanisms.

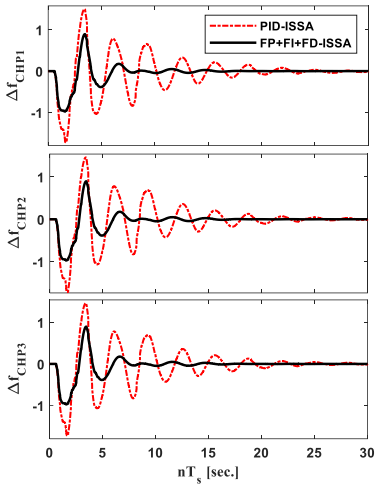

Fig. 12 The deviations of frequency at the CHP buses.

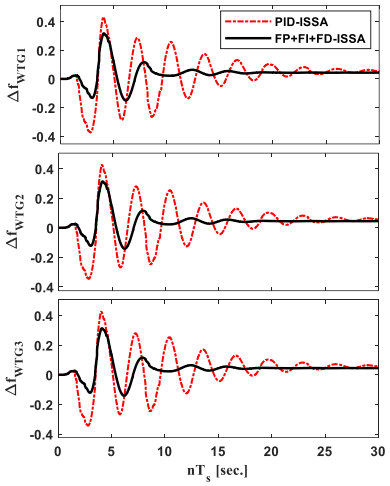

Fig. 13 The deviations of frequency at the WTG buses.

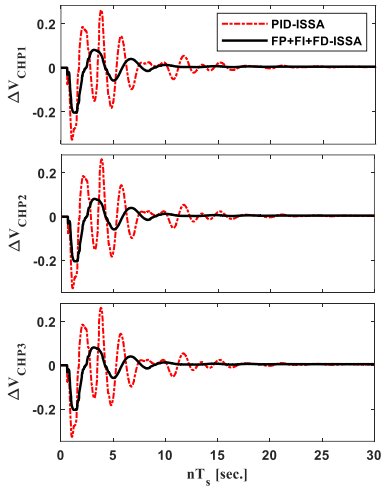

Fig. 14 The deviations of voltage at the CHP buses.

the FP+FI+FD controller is inferred from simulation results compared to the PID control method.

Results show that the dynamics of the MEG is improved in terms of overshoot /undershoot, increasing the speed of the oscillation damping, and the complete removal of the steady-state error. This is the undeniable fact that the optimal tuning of the FP+FI+FD controller parameters makes the different parts of it consistent together and each of them performs their tasks correctly. Furthermore, the total production of active and reactive powers of MEG during fault occurrence is shown in Fig. 16. The active power remains constant after some oscillations. Wherever it is evident that the FP+FI+FD controller is superb in damping the oscillations compared to the traditional PID controller.

5.2 Discussion

The previous section has shown the ability of the FP+FI+FD controller to be clear compared to the traditional PID method. In this section, firstly, the results of the previous section are proved using statistical analysis of time-domain results. Then, the MEG stability is discussed in the presence of FP+FI+FD controller.

5.2.1 Time Domain Analysis

In this section, in order to more highlighting the capabilities of the proposed ISSA based FP+FI+FD mechanism, time-domain analyses are performed. For this aim, suitable time-domain criteria, such as overshoot (*OS*), undershoot (*US*), settling time (*Ts*), integral of time multiplied by absolute error (*ITAE*) and integral of squared error (*ISE*) have been calculated. The results are tabulated in Table 3. It should be noted that for the calculation of ITAE and ISE, Eqs. (22) and (23) are used.

$$ITAE_{\Psi} = \sum_{n=1}^{30000} n \times T_s \times \Psi(n) \tag{22}$$

$$ISE_{\Psi} = \sum_{n=1}^{30000} [\Psi(n)]^2 \tag{23}$$

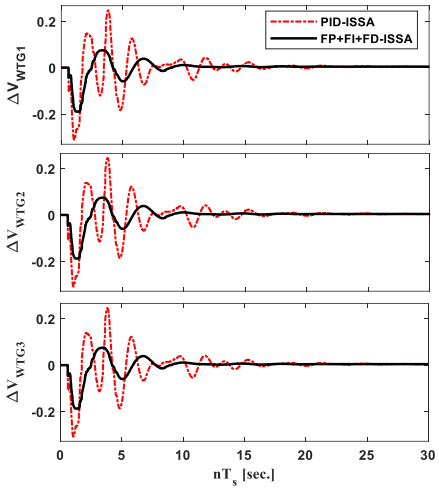

Fig. 15 The deviations of voltage at the WTG buses.

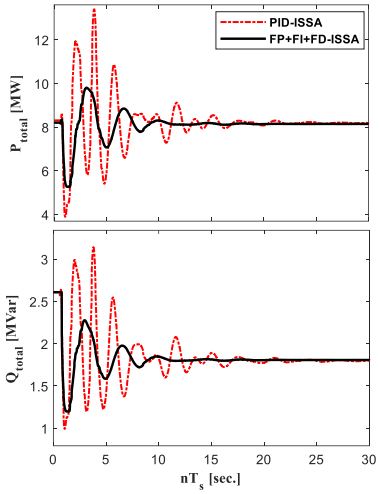

Fig. 16 Active and reactive powers of the MEG under fault condition.

Table 3 Time domain performance indices for ISSA based FP+FI+FD and classical PID controllers.

Frequency							
Signal		Δf_{CHP1}	Δf_{CHP2}	Δf_{CHP3}	Δf_{WTG1}	Δf_{WTG2}	Δf_{WTG3}
OS	PID	1.4991	1.4601	1.4601	0.4313	0.4254	0.4254
	FP+FI+FD	0.8942	0.8956	0.8956	0.3172	0.3134	0.3135
US	PID	1.7220	1.7197	1.7197	0.3731	0.3458	0.3431
	FP+FI+FD	0.9763	0.9715	0.9715	0.1501	0.1415	0.1411
Ts	PID	20	20	20	26	28	28
	FP+FI+FD	10	10	10	15	14	15
ITAE	PID	62.1966	61.4553	61.4553	54.0451	54.4802	54.5165
	FP+FI+FD	10.8434	10.8190	10.8190	37.3142	38.2486	38.3166
ISE	PID	6.62567	6.60094	6.60094	0.63903	0.60035	0.597715
	FP+FI+FD	1.757922	1.747188	1.747188	0.197731	0.1970426	0.19726161
Voltage							
Signal		ΔV_{CHP1}	ΔV_{CHP2}	ΔV_{CHP3}	ΔV_{WTG1}	ΔV_{WTG2}	ΔV_{WTG3}
OS	PID	26.2274	26.1906	26.1906	24.7240	24.46034	24.51265
	FP+FI+FD	8.1367	8.1360	8.1360	7.47912	7.45826	7.48861
US	PID	32.66225	32.68944	32.68944	31.02750	30.794369	30.77497
	FP+FI+FD	20.34233	20.35127	20.35127	18.98489	18.737909	18.72321
Ts	PID	15	16	15	16	16	16
	FP+FI+FD	9	9	9	9	9	9
ITAE	PID	7.37690	7.37464	7.37464	7.13375	7.03692	7.03992
	FP+FI+FD	5.16348	5.16710	5.16710	4.63883	4.57343	4.57359
ISE	PID	0.1465676	0.1465289	0.146528	0.1260056	0.12303663	0.1230699
	FP+FI+FD	0.0439209	0.0439544	0.043954	0.0396697	0.03909224	0.0391328

where n is an integer, T_s is sampling time and considered equal to 1ms in this paper, and Ψ refers to the corresponding signal i.e. Δf_i and ΔV_i signals.

From Table 3 it is clear that the FP+FI+FD controller compared to the PID method has enhanced the overshoot of frequency signal approximately 50% and 25% at CHP and WTG buses, respectively. These improvements are 70% at both CHP and WTG generation buses in the perspective of the voltage signal. Also, the undershoot index is improved at least 45% at all generation buses for both frequency and voltage signals. The maximum and minimum enhancements in settling time are 50% and 43%, respectively. Likewise, the ITAE criterion is ameliorated at least 28% and utmost 83% using FP+FI+FD control mechanism compared to the classical PID method. As a result, the FP+FI+FD controller, thanks to its flexible structure, which is derived from the mixing the fuzzy logic and PID controller features, can improve the MEG oscillations in the shortest possible time, and ensures the voltage and frequency stability. It should be noted that the optimal configuration of the control parameters and the range of fuzzy membership functions is of particular importance. In this paper, an improved version of the SSA, which is more suitable for complex-engineering problems, has been used.

5.2.2 Stability Analysis

The stability analysis of the system with the controller

Table 4 The value of α_1 for different ICs of FP+FI+FD control method.

IC regions	Value of α_1
IC 1 & *IC* 3	$\left\|\frac{LK_P(K_{P2}-K_{P1})}{2(2L-K_{P1}M_e)}+\frac{LK_I(\mathrm{T}K_{I2}+K_{I1})}{2T(2L-K_{I1}M_e)}+\frac{LK_D(\mathrm{T}K_{D2}-K_{D1})}{2T(2L-K_{D2}M_e)}\right\|$
IC 2 & *IC* 4	$\left\|\frac{LK_P(K_{P2}-K_{P1})}{2(2L-K_{P2}M_{\Delta e})}+\frac{LK_I(\mathrm{T}K_{I2}+K_{I1})}{2T(2L-K_{I2}M_r)}+\frac{LK_D(\mathrm{T}K_{D2}-K_{D1})}{2T(2L-K_{D1}M_r)}\right\|$
IC 5	$\left\|\frac{K_PK_{P2}}{2}+\frac{K_IK_{I2}}{2T}-\frac{K_DK_{D1}}{2T}\right\|$
IC 6	0
IC 7	$\left\|\frac{K_IK_{I1}}{2}+\frac{K_DK_{D2}}{2}-\frac{K_PK_{P1}}{2}\right\|$
IC 8	0
IC 9	$\left\|\frac{K_PK_{P2}}{2}+\frac{K_IK_{I2}}{2T}-\frac{K_DK_{D1}}{2T}\right\|$
IC 10	0
IC 11	$\left\|\frac{K_IK_{I1}}{2}+\frac{K_DK_{D2}}{2}-\frac{K_PK_{P1}}{2}\right\|$
IC 12	0

Table 5 The value of α_1 and $\alpha_1 \times R$ for all 12 IC regions of FP+FI+FD controller applied to the AVR system.

Output signal		IC regions of FP+FI+FD control method									
		IC 1 & *IC* 3	*IC* 2 & *IC* 4	*IC* 5	*IC* 6	*IC* 7	*IC* 8	*IC* 9	*IC* 10	*IC* 11	*IC* 12
Δf_1	α_1	0.2032	0.2048	0.6384	0	0.2320	0	0.6384	0	0.2320	0
	$\alpha_1 \times \|\|R\|\|_{max}$	10.02	10.09	31.46	0	11.44	0	31.46	0	11.44	0
Δf_2	α_1	0.2032	0.2048	0.6384	0	0.2320	0	0.6384	0	0.2320	0
	$\alpha_1 \times \|\|R\|\|_{max}$	10.02	10.09	31.46	0	11.44	0	31.46	0	11.44	0
Δf_3	α_1	0.2032	0.2048	0.6384	0	0.2320	0	0.6384	0	0.2320	0
	$\alpha_1 \times \|\|R\|\|_{max}$	10.02	10.09	31.46	0	11.44	0	31.46	0	11.44	0
ΔV_1	α_1	0.0338	0.0339	0.1200	0	0.0525	0	0.1200	0	0.0525	0
	$\alpha_1 \times \|\|R\|\|_{max}$	1.66	1.67	5.92	0	2.59	0	5.92	0	2.59	0
ΔV_2	α_1	0.0338	0.0339	0.1200	0	0.0525	0	0.1200	0	0.0525	0
	$\alpha_1 \times \|\|R\|\|_{max}$	1.66	1.67	5.92	0	2.59	0	5.92	0	2.59	0
ΔV_3	α_1	0.0338	0.0339	0.1200	0	0.0525	0	0.1200	0	0.0525	0
	$\alpha_1 \times \|\|R\|\|_{max}$	1.66	1.67	5.92	0	2.59	0	5.92	0	2.59	0

after the optimal design can ensure the desired performance of the controller from the perspective of the frequency domain. However, the stability analysis of complex systems with the presence of fuzzy controller is very difficult [36]. Although, FP+FI+FD controller stability analysis for different systems is investigated in [21, 25]. The FP+FI+FD controller stability analysis has finally been expressed as a theorem as follows [25]:

Theorem 1: If the process under control denoted by *R*, the sufficient condition for the nonlinear FP+FI+FD control system is to be stable are:

1) The process under control has a bounded norm (gain) ie. $\|R\|_\infty < \infty$.
2) The parameters of FP+FI+FD controller satisfy Eq. (17).

$$\alpha_1 \|R\| < \infty \tag{24}$$

where α_1 is different for any input combination (IC) regions of FP+FI+FD controller (see [21, 25]), and given in Table 4.

In Table 5, M_e is maximum magnitude of error, $M_{\Delta e} = 2M_e$, $M_r = 2M_e/Ts$.

Since the current MEG test system is a multi-input-multi-output (MIMO) system, then the H_∞ norm is considered equal to the largest singular value across the frequencies [37]. Given that six FP+FI+FD controllers have been studied in the MEG test system, the proposed MIMO system is considered as six separate MISO systems, and the corresponding α_1 values are calculated. The results are tabulated in Table 5. It should be noted that the H_∞ of the proposed MIMO MEG test system is calculated by (18) [21, 37].

$$\|MEG(z)\|_\infty = \max_{\theta\in[0,\pi]} \left|MEG\left(e^{j\theta}\right)\right|$$
$$\Rightarrow \|MEG(z)\|_\infty = 49.28319 < \infty \quad (25)$$

It can be concluded that according to **Theorem 1** and using the result obtained in (18) and the data provided in Table 6, the sufficient conditions for the voltage and frequency stability of the proposed MEG are satisfied.

6 Conclusions

The primary objective of this paper was to model and optimize the parallel FuzzyP+FuzzyI+FuzzyD (FP+FI+FD) controller for simultaneous control of the voltage and frequency of a micro-energy-grid in islanded mode. The FP+FI+FD controller has three parallel branches, each of which has a specific task. Finally, as its name suggests, the final output of the controller is derived from the algebraic summation of the outputs of these three branches. The proposed control strategy is adaptive and fast inherently, due to combining the features of fuzzy logic with PID control method. This paper was attempted to determine the optimal control gains and Fuzzy membership functions of the FP+FI+FD controller using an improved Salp swarm algorithm (ISSA) to achieve its optimal dynamic response. The time-domain simulations were carried out in order to prove the superb dynamic response of the proposed FP+FI+FD controller compared to the PID control method. In addition, a multi-input-multi-output (MIMO) stability analysis was performed to ensure the robust control characteristic of the proposed parallel fuzzy controller. Finally, according to the simulation results and discussion analysis, the superb performance of the proposed control method can be realized evidently.

Acknowledgment

This research was supported by the University of Mohaghegh Ardabili Research Development Fund.

Appendix A

Reduced Y_{bus} matrix is shown in (A.1).

Appendix B

Load flow results and initial conditions are tabulated in Tables B.1 and B.2.

$$Y_{bus}^{red} = \begin{bmatrix} +1.0157 - j1.1498 & -0.3961 + j0.4972 & -0.3961 + j0.4972 & -0.0928 + j0.0721 & -0.0573 + j0.0426 & -0.0535 + j0.0355 \\ -0.3961 + j0.4972 & +1.0157 - j1.1498 & -0.3961 + j0.4972 & -0.0928 + j0.0721 & -0.0573 + j0.0426 & -0.0535 + j0.0355 \\ -0.3961 + j0.4972 & -0.3961 + j0.4972 & +1.0157 - j1.1498 & -0.0928 + j0.0721 & -0.0573 + j0.0426 & -0.0535 + j0.0355 \\ -0.0928 + j0.0721 & -0.0928 + j0.0721 & -0.0928 + j0.0721 & +0.4332 - j0.3624 & -0.0742 + j0.0785 & -0.0742 + j0.0785 \\ -0.0573 + j0.0426 & -0.0573 + j0.0426 & -0.0573 + j0.0426 & -0.0742 + j0.0785 & +0.3983 - j0.3381 & -0.1458 + j0.1328 \\ -0.0535 + j0.0355 & -0.0535 + j0.0355 & -0.0535 + j0.0355 & -0.0703 + j0.0670 & -0.1458 + j0.1328 & +0.3824 - j0.3049 \end{bmatrix} \times 10^2 \quad (A.1)$$

Table B.1 Power flow results for MEG at the given operating condition.

Bus	$\|V\|$	θ	P_g	Q_g
1	1	0	3.07	0.69
2	1	-0.5	2.9	0.67
3	1	-0.5	2.9	0.67
4	0.98	-11.34	0.1	0
5	0.97	-11.35	0.1	0
6	0.97	-11.35	0.1	0

Table B.2 The initial condition for MEG at the given operating condition.

Parameter	CHP 1	CHP 2	CHP3	WTG 1	WTG 2	WTG 3
I_{a0}	3.147	2.976	2.976	0.090	0.901	0.090
Φ_0	-0.221	-0.236	-0.236	-0.198	-0.198	-0.198
E_{q0}	1.386	1.369	1.369	1.122	1.122	1.122
δ_0	0.519	0.499	0.499	0	0	0
I_{d0}	-2.121	-1.996	-1.996	-0.018	-0.018	-0.018
I_{q0}	2.324	2.208	2.208	0.088	0.088	0.088
V_{d0}	-0.496	-0.487	-0.487	-0.218	-0.219	-0.219
V_{q0}	0.868	0.874	0.874	1.088	1.088	1.088
E'_{d0}	0.278	0.264	0.264	0.011	0.011	0.011
E'_{q0}	1.069	1.071	1.071	0.002	0.002	0.002
T_{e0}	3.044	2.971	2.971	0.122	0.122	0.122
T_{m0}	3.044	2.971	2.971	0.122	0.122	0.122

References

[1] K. W. Joung, T. Kim, and J. Park, "Decoupled frequency and voltage control for stand-alone microgrid with high renewable penetration," *IEEE Transactions on Industry Applications*, Vol. 55, pp. 122–133, 2019.

[2] Y. Xu, H. Sun, W. Gu, Y. Xu, and Z. Li, "Optimal distributed control for secondary frequency and voltage regulation in an islanded microgrid," *IEEE Transactions on Industrial Informatics*, Vol. 15, pp. 225–235, 2019.

[3] H. Shayeghi and A. Younesi, "Mini/Micro-grid adaptive voltage and frequency stability enhancement using Q-learning mechanism," *Journal of Operation and Automation in Power Engineering*, Vol. 7, No. 1, pp. 107–118, May 2019.

[4] R. Heydari, T. Dragicevic, and F. Blaabjerg, "High-bandwidth secondary voltage and frequency control of VSC-based AC microgrid," *IEEE Transactions on Power Electronics*, pp. 1–1, 2019.

[5] Y. Hirase, K. Abe, K. Sugimoto, K. Sakimoto, H. Bevrani, and T. Ise, "A novel control approach for virtual synchronous generators to suppress frequency and voltage fluctuations in microgrids," *Applied Energy*, Vol. 210, pp. 699–710, 2018.

[6] X. Chen, Y. Hou, and S. Y. R. Hui, "Distributed control of multiple electric springs for voltage control in microgrid," I*EEE Transactions on Smart Grid*, Vol. 8, pp. 1350–1359, 2017.

[7] Y. Dong, X. Xie, W. Shi, B. Zhou, and Q. Jiang, "Demand-response based distributed preventive control to improve short-term voltage stability," *IEEE Transactions on Smart Grid*, Vol. 9, No. 5, pp. 4785–4795, 2017.

[8] H. Zhao, M. Hong, W. Lin, and K. A. Loparo, "Voltage and frequency regulation of microgrid with battery energy storage systems," *IEEE Transactions on Smart Grid*, Vol. 10, No. 1, pp. 414–424, 2017.

[9] F. Gao, S. Bozhko, A. Costabeber, C. Patel, P. Wheeler, C. I. Hill, and G. Asher, "Comparative stability analysis of droop control approaches in voltage-source-converter-based DC microgrids," *IEEE Transactions on Power Electronic*s, Vol. 32, No. 3, pp. 2395-2415, 2016.

[10] A. Hajizadeh, "Robust power control of microgrid based on hybrid renewable power generation systems," *Iranian Journal of Electrical and Electronic Engineering*, Vol. 9, No. 1, pp. 58–66, 2013.

[11] H. Shayeghi and A. Ghasemi, "Improvement of frequency fluctuations in microgrids using an optimized fuzzy P-PID controller by modified multi objective gravitational search algorithm," *Iranian Journal of Electrical and Electronic Engineering*, Vol. 12, No. 4, pp. 241–256, 2016.

[12] A. A. Khodadoost Arani, B. Zaker, and G. B. Gharehpetian, "A control strategy for flywheel energy storage system for frequency stability improvement in islanded microgrid," *Iranian Journal of Electrical and Electronic Engineering*, Vol. 13, No. 1, pp. 10–21, 2017.

[13] J. W. Simpson-Porco, F. Dörfler, and F. Bullo, "Voltage stabilization in microgrids via quadratic droop control," *IEEE Transactions on Automatic Control*, Vol. 62, No. 3, pp. 1239–1253, 2017.

[14] F. Asghar, M. Talha, and S. Kim, "Robust frequency and voltage stability control strategy for standalone AC/DC hybrid microgrid," *Energies*, Vol. 10, No. 6, p. 760, 2017.

[15] A. A. Abass and M. U.-D. Mufti, "SimPower-based analysis and design of a hybrid wind–diesel-superconducting magnetic energy storage system for simultaneous frequency and voltage control," *Wind Engineering*, Vol. 43, No. 6, pp. 596–608, 2019.

[16] X. Li, H. Wen, Y. Hu, and L. Jiang, "A novel beta parameter based fuzzy-logic controller for photovoltaic MPPT application," *Renewable Energy*, Vol. 130, pp. 416–427, 2019.

[17] Y. Bai and Z. S. Roth, "Interval type-2 fuzzy logic controllers," in *Classical and Modern Controls with Microcontrollers: Design, Implementation and Applications*, Cham: Springer International Publishing, pp. 549-579, 2019.

[18] A. Ali, L. Abbas, M. Shafiq, A. K. Bashir, M. K. Afzal, H. B. Liaqat, M. H. Siddiqi, and K. S. Kwak, "Hybrid fuzzy logic scheme for efficient channel utilization in cognitive radio networks," *IEEE Access*, Vol. 7, pp. 24463–24476, 2019.

[19] M. Nabipour, M. Razaz, S. G. Seifossadat, and S. S. Mortazavi, "A novel adaptive fuzzy membership function tuning algorithm for robust control of a PV-based dynamic voltage restorer (DVR)," Eng*ineering Applications of Artificial Intelligence*, Vol. 53, pp. 155–175, 2016.

[20] N. J. Vinoth Kumar and M. M. Thameem Ansari, "A new design of dual mode Type-II fuzzy logic load frequency controller for interconnected power systems with parallel AC–DC tie-lines and capacitor energy storage unit," *International Journal of Electrical Power & Energy Systems*, Vol. 82, pp. 579–598, 2016.

[21] H. Shayeghi, A. Younesi, and Y. Hashemi, "Optimal design of a robust discrete parallel FP+FI+FD controller for the automatic voltage regulator system," *International Journal of Electrical Power & Energy Systems*, Vol. 67, pp. 66–75, 2015.

[22] V. Kumar and A. P. Mittal, "Parallel fuzzy P+fuzzy I+fuzzy D controller: Design and performance evaluation," *International Journal of Automation and Computing*, Vol. 7, pp. 463–471, 2010.

[23] H. Shayeghi and A. Younesi, "A robust discrete FuzzyP+FuzzyI+FuzzyD load frequency controller for multi-source power system in restructuring environment," *Journal of Operation and Automation in Power Engineering*, Vol. 5, No. 1, pp. 61–74, 2017.

[24] S. Mirjalili, A. H. Gandomi, S. Z. Mirjalili, S. Saremi, H. Faris, and S. M. Mirjalili, "Salp swarm algorithm: A bio-inspired optimizer for engineering design problems," *Advances in Engineering Software*, Vol. 114, pp. 163–191, 2017.

[25] V. Kumar, B. C. Nakra, and A. P. Mittal, "Some investigations on fuzzyP+fuzzyI+fuzzy D controller for non-stationary process," *International Journal of Automation and Computing*, Vol. 9, No. 5, pp. 449–458, 2012.

[26] D. Liu, J. Wu, K. Lin, and M. Wu, "Planning of multi energy-type micro energy grid based on improved kriging model," *IEEE Access*, Vol. 7, pp. 14569–14580, 2019.

[27] N. Faridnia, D. Habibi, S. Lachowicz, and A. Kavousifard, "Optimal scheduling in a microgrid with a tidal generation," *Energy*, Vol. 171, pp. 435–443, 2019.

[28] P. Mahat, Z. Chen, and B. Bak-Jensen, "Control and operation of distributed generation in distribution systems," *Electric Power Systems Research*, Vol. 81, pp. 495–502, 2011.

[29] D. Yu, H. Zhu, W. Han, and D. Holburn, "Dynamic multi agent-based management and load frequency control of PV/Fuel cell/wind turbine/CHP in autonomous microgrid system," *Energy*, Vol. 173, pp. 554–568, 2019.

[30] P. Kundur, N. J. Balu, and M. G. Lauby, *Power system stability and control*. New York: McGraw-hill, 1994.

[31] A. Younesi, H. Shayeghi, and M. Moradzadeh, "Application of reinforcement learning for generating optimal control signal to the IPFC for damping of low-frequency oscillations," *International Transactions on Electrical Energy Systems*, Vol. 28, No. 2, p. e2488, 2018.

[32] V. Kumar and A. Mittal, "Parallel fuzzy P+fuzzy I+fuzzy D controller: Design and performance evaluation," *International Journal of Automation and Computing*, Vol. 7, pp. 463–471, 2010.

[33] R. Eberhart and J. Kennedy, "Particle swarm optimization," in *Proceedings of the IEEE International Conference on Neural Networks*, Vol.4, pp. 1942–1948, 1995.

[34] T. C. Chin and X. M. Qi, "Genetic algorithms for learning the rule base of fuzzy logic controller," *Fuzzy Sets and Systems*, Vol. 97, No. 1, pp. 1–7, 1998.

[35] D. Mondal, A. Chakrabarti, and A. Sengupta, *Power system small signal stability analysis and control*. Elsevier Imprint: Academic Press Publication, 2014.

[36] F. Ni, L. Yan, J. Liu, M. Shi, J. Zhou, and X. Chen, "Fuzzy logic-based virtual capacitor adaptive control for multiple HESSs in a DC microgrid system," *International Journal of Electrical Power & Energy Systems*, Vol. 107, pp. 78–88, 2019.

[37] The MathWorks Inc., "Matlab programming," 2018. Available at: http://www.mathworks.com.

H. Shayeghi received the B.Sc. and M.S.E. degrees in Electrical and Control Engineering in 1996 and 1998, respectively. He received his Ph.D. degree in Electrical Engineering from Iran University of Science and Technology, Tehran, Iran in 2006. Currently, he is a Full Professor in Technical Engineering Department of University of Mohaghegh Ardabili, Ardabil, Iran. His research interests are in the application of robust control, artificial intelligence and heuristic optimization methods to power system control design, operation and planning and power system restructuring. He has authored and co-authored of 5 books in Electrical Engineering area all in Farsi, one book and two book chapters in international publishers and more than 330 papers in international journals and conference proceedings. Also, he collaborates with several international journals as reviewer boards and works as editorial committee of three international journals. He has served on several other committees and panels in governmental, industrial, and technical conferences. He was selected as distinguished researcher of the University of Mohaghegh Ardabili several times. In 2007 and 2010 he was also elected as distinguished researcher in engineering field in Ardabil province of Iran. Furthermore, he has been included in the Thomson Reuters' list of the top one percent of most-cited technical Engineering scientists in 2015 and 2016, respectively. Also, he is a member of Iranian Association of Electrical and Electronic Engineers (IAEEE) and Senior member of IEEE.

A. Younesi received the B.Sc and M.S.E degrees both in Electrical Engineering from Technical Engineering Department of the Mohaghegh Ardabili University, Ardabil, Iran in 2012 and 2015, respectively. Currently He is a PhD. student in Technical Engineering Department of the University of Mohaghegh Ardabili, Ardabil, Iran. His areas of interest are Power system resiliency, Microgrid control and management, application of artificial intelligence in power system automation and control, application of reinforcement learning to power system control, fuzzy systems, heuristic optimization in power system control. He is a student member of Iranian Association of Electrical and Electronic Engineers (IAEEE) and IEEE.